A Novel Reactive Liquid Rubber with Maleimide End Groups for the Toughening of Unsaturated Polyester Resins

M. ABBATE,[1] E. MARTUSCELLI,[1] P. MUSTO,[1] G. RAGOSTA,[1,*] and M. LEONARDI[2]

[1]National Research Council of Italy, Institute of Research and Technology of Plastic Materials, via Toiano 6, 80072 Arco Felice (NA), Italy; [2]Lonza SpA, S. Giovanni Valdarno (AR), Italy

SYNOPSIS

An amino-terminated butadiene–acrylonitrile copolymer was chemically modified into a maleimido-terminated rubber and was used as a toughening agent for an unsaturated polyester resin. The reactive rubber was characterized by Fourier transform infrared spectroscopy. The mechanical and fracture properties of the blends containing the unmodified and the modified rubbers were investigated. Furthermore, a morphological analysis was carried out by scanning and transmission electron microscopy. A substantial enhancement of toughness was found when the modified rubber was used in place of the plain copolymer. © 1996 John Wiley & Sons, Inc.

INTRODUCTION

Unsaturated polyester (UP) resins represent one of the most important matrices for composite applications. They are particularly useful in sheet-molding compounds (SMC) and bulk-molding compounds (BMC) for manufacturing automotive parts.[1] Like other thermosets, UP resins are blended with several additives to enhance their properties. For example, the polymerization shrinkage of the material during curing may cause molding problems such as poor surface quality, warpage, and difficult dimension control. Most of these problems are eliminated using low-profile additives like poly(methyl metacrylate) and poly(vinyl acetate).[2,3] Moreover, the UP resins are limited by their brittleness, especially when good impact behavior is required. To overcome this limitation, blending with liquid rubbers has been widely used,[4–6] often with limited success. The critical point of this approach is the limited solubility of the rubbery component in the unreacted resin as well as the poor chemical reactivity of the rubber toward the polyester functionalities. We have thus chemically modified commercially available liquid rubbers so as to enhance their reactivity toward the UP end groups. In particular, in a previous contribution,[7] a hydroxyl-terminated polybutadiene was transformed into an isocyanate-terminated rubber and the isocyanate functionalities were reacted with the hydroxyl end groups of the UP resin prior to the curing process. Interesting results in terms of toughness and morphology were obtained on this blend system. In the present work, a further modification of a commercial liquid rubber is described: An amino-terminated butadiene–acrylonitrile copolymer is transformed in maleimide-terminated rubber; these functionalities are able to interact chemically with the other unsaturations present in the UP resin during the curing process. The molecular characterization of such a modified reactive rubber was accomplished by Fourier transform infrared spectroscopy (FTIR). The mechanical properties of the cured materials were studied at low and high rates of deformation, using the linear elastic fracture mechanics approach. The results of this analysis were correlated eventually with the morphology of the samples investigated by transmission and by scanning electron microscopy.

EXPERIMENTAL

Materials

The UP resin was an uncured, unsaturated polyester kindly supplied by Lonza S.p.A. The resin was available as a solution containing 35% of styrene.

* To whom correspondence should be addressed.

Journal of Applied Polymer Science, Vol. 62, 2107–2119 (1996)
 CCC 0021-8995/96/122107-13

The acid number of the prepolymer, defined as the mg of KOH used for the titration of 1 g of prepolymer, was 19.2. The OH number, obtained by titration of the excess acetic anhydride used to fully esterify the hydroxyl groups, was 53.4. This corresponds to 0.34 mmol of COOH groups and 0.95 mmol of OH groups per gram of resin. In the UP formulation, 0.1% by weight of hydroquinone was employed as inhibitor to prevent premature curing. Benzoyl peroxide (BOP) was the radical initiator and was recrystallized twice from absolute ethanol before use.

The liquid rubber was an amino-terminated butadiene–acrylonitrile copolymer (ATBN) produced by Goodrich. The acrylonitrile content was 18% and the molecular weight $\overline{M_n}$ = 3600.

Preparation of Maleimide-terminated Copolymer

The imidation reaction was carried out in two steps: First maleamic acid was formed, followed by cyclization through dehydration with acetic anhydride/sodium acetate. In a round-bottom flask equipped with a nitrogen inlet and a condenser, 30.0 g of ATBN were dissolved in 250 mL of chloroform; upon complete dissolution, the temperature was increased to 65°C and 7.5 g of maleic anhydride was added. The solution, initially clear, gradually became turbid, indicating a reduced solubility of the maleamic acid intermediate in chloroform. After 5 h, 15.6 g of acetic anhydride and 0.10 g of sodium acetate were added, and the mixture was kept at 65°C for additional 3 h. At the end of this period, the solution became homogeneous again, and its color changed from white ivory to brown-red. At this point, the solution was cooled and filtered and the solvent was eliminated in a rotovapor. Further purification was carried out by vacuum drying for 24 h at 70°C up to the constant weight of the product.

Preparation Procedures of a Typical UP/Rubber Blend

Seven grams of rubber (ATBN or ITBN) were mixed with 63 g of UP resin for 30 min under vigorous mechanical stirring. After the homogenization of the mixture, 1.26 g of the radical initiator BOP were added, continuing the mixing for additional 5 min. At this stage, the reactive mixture was degassed under vacuum for 2 min and poured into a glass mold which was immersed in a thermostatic bath at 50°C for 2 h. The cure was continued for 10 h at 70°C and was followed by a postcure at 100°C for 2 h. This procedure describes the preparation of a 90/10 UP/rubber blend. The compositions and codes of the various investigated blends are reported in Tables I and II.

Techniques

FTIR spectra were collected on thin films obtained by sandwiching a drop of the reactive rubber between two KBr windows. The spectra were obtained at a resolution of 2 cm^{-1} with a Perkin-Elmer System 2000 spectrometer equipped with a deuterated tryglicine sulfate detector (DTGS) and a germanium/KBr beam splitter. The recorded wavenumber range was 4000–400 cm^{-1}; the interferogram data were Fourier transformed using a triangular apodization function. The frequency scale was internally calibrated to an accuracy of ± 0.02 cm^{-1} using a He—Ne laser.

Uniaxial compressive tests were made on samples 12 mm long, 6.0 mm wide, and 4.0 mm thick using an Instron mechanical tester at ambient temperature and at a crosshead speed of 1 mm/min. Three-point bending specimens were used to perform fracture tests at room temperature at low and high strain rates. The low strain rate measurements were carried out on an Instron apparatus at a crosshead speed of 1 mm/min. The high strain rate tests were performed on a Charpy instrumented pendulum at room temperature and at an impact speed of 1 m/s. For both the tests, samples (60 × 6.0 × 4.0 mm) were cut from sheets of the cured materials and then sharply notched. The fracture data were analyzed according to the concepts of linear elastic fracture mechanics.[8]

The critical stress intensity factor, K_c, was calculated using the following equation:

$$K_c = \sigma Y \sqrt{a} \tag{1}$$

where σ is the nominal stress at the onset of crack propagation; a, the initial crack length; and Y, a calibration factor depending upon the specimen geometry. For three-point bending specimens, Y is given by Brown and Srawley.[9] For the determination

Table I Codes and Compositions of the UP/ATBN Blends

Code	UP (wt %)	ATBN (wt %)
B0	100	—
B4	96	4
B8	92	8
B10	90	10
B15	85	15

Table II Codes and Compositions of the UP/ITBN Blends

Code	UP (wt %)	ITBN (wt %)
C4	96	4
C8	92	8
C10	90	10
C15	85	15

of the critical strain energy release rate, G_c, the following equation was used:

$$G_c = \frac{U}{BW\phi} \tag{2}$$

where U is the fracture energy; B and W, the thickness and the width of the specimen respectively; and ϕ, a calibration factor which depends on the length of the notch and the size of the sample. Values of ϕ were taken from Plati and Williams.[10]

Ultrathin sections of rubber-modified UP resin were examined using a Philips transmission electron microscope (TEM). Specimens were first trimmed on an ultramicrotome to form truncate pyramids. The blocks were then stained by immersion in a 2 w/w % aqueous solution of osmium tetroxide with an equal volume of tetrahydrofuran. Immersion of 40 min was found to give a stained layer around 20 μm deep, from which several sections were cut, around 100 nm thick, using a diamond knife. These were collected on a 3 mm copper grid, ready for insertion in the TEM.

Fractured surfaces were coated with a thin layer of a gold–palladium alloy and then examined by scanning electron microscopy (SEM). Prior to SEM examination, some samples were etched with boiling CH_2Cl_2 to selectively remove the rubber component.

RESULTS AND DISCUSSION

Spectroscopic Characterization of the Reactive Rubber

To improve the reactivity of the amino-terminated butadiene–acrylonitrile copolymer (ATBN) toward the UP matrix, the $-NH_2$ end groups of the liquid rubber were chemically transformed into maleimide groups. The $-NH_2$ groups on ATBN were obtained by reacting a carboxyl-terminated butadiene–acrylonitrile copolymer with methylpentamethylene diamine. Thus, the chemical structure of the ATBN terminal groups is the following:

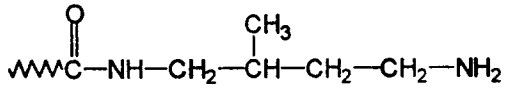

The reaction scheme for the preparation of the maleimido-terminated copolymer (ITBN) is the following:

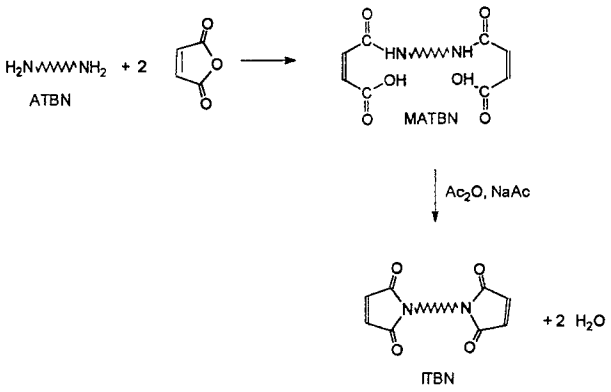

The reaction is carried out in chloroform as the solvent and proceeds in two steps. First, maleamic acid is formed by reacting the $-NH_2$ end groups with a stoichiometric amount of maleic anhydride at room temperature. Then, this intermediate (MATBN) is cyclized by adding to the solution acetic anhydride and sodium acetate. It has been found that the cyclization reaction also proceeds at temperatures above 100°C (to be discussed later).

In Figure 1 are compared the FTIR transmission spectra of ATBN [Fig. 1(A)], MATBN [Fig. 1(B)], and ITBN [Fig. 1(C)]. In the discussion below, we focus attention on the spectral regions where the amide and carbonyl groups display their characteristic absorptions (3600–3000 cm^{-1} for the ν_{NH} vibrations and 1800–1550 cm^{-1} for the amide modes).

The ATBN spectrum displays a broad, irregularly shaped absorption centered at 3300 cm^{-1} which can be attributed to the ν_{NH} modes of the amide linkages and of the primary amine in the terminal groups. This peak displays a higher-frequency shoulder at approximately 3385 cm^{-1}. The low-frequency component is due to hydrogen-bonded N—H groups, while the high-frequency shoulder is due to free amidic N—H. Typical amide absorptions are detected also in the carbonyl frequency range [see Fig. 2(A)]. In particular, two peaks centered at about 1650 and 1545 cm^{-1} (amide modes I and II) are observed. Unlike the essentially isolated NH stretching, these two modes are more complex vibrations.

In particular, the amide I mode is predominantly a C=O stretching, but has significant contributions from a C—N stretching and a C—C—N defor-

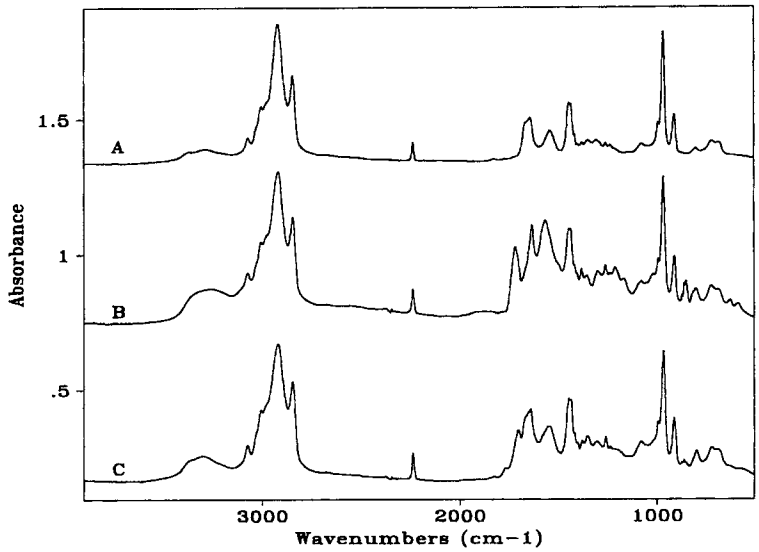

Figure 1 FTIR transmission spectra in the frequency range 4000–400 cm^{-1} of (A) ATBN, (B) MATBN, and (C) ITBN.

mation.[11] This mode is conformationally sensitive and has been widely used to detect the different conformations in polypeptides and proteins.[12] In the ATBN spectrum, the amide I band clearly displays two unresolved components at 1670 and at 1645 cm^{-1}. The two components are assigned to hydrogen-bonded carbonyls (at 1645 cm^{-1}) and to carbonyls not involved in specific intermolecular interactions (at 1675 cm^{-1}). Thus, in the system under investigation, the following type of hydrogen-bonding interactions takes place:

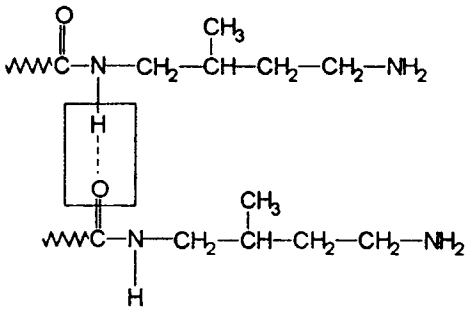

Hydrogen bonding involving carbonyls as acceptors and $-NH_2$ groups as donors cannot be entirely ruled out.

Assuming that the absorptivities of interacting and noninteracting carbonyls do not differ substantially, as it is generally the case, in the ATBN copolymer at room temperature, the population of interacting C=O groups prevails over the population of noninteracting groups.

Well-defined differences are observed in the MATBN spectrum with respect to the spectrum of the parent copolymer. In particular, in the NH stretching region, the peak intensity increases substantially; the absorption is now centered at 3275 cm^{-1} and remains rather broad. This effect is due to the presence, in the MATBN spectrum, of the contribution of the newly formed NH groups of the maleamic acid moieties, which further complicate the ν_{NH} region.

The carbonyl region of the MATBN spectrum is also very different from that of the parent copolymer [see Fig. 2(B)]: A new, highly symmetrical peak centered at 1719 cm^{-1} is observed, which is assigned to the $\nu_{C=O}$ vibration of the carboxyl groups in the maleamic acid moiety. A further absorption is found at 1635 cm^{-1}, while the peak originally centered at 1545 cm^{-1} in the ATBN spectrum strongly increases in intensity and shifts at 1576 cm^{-1}. This doublet is still due to amide bands I and II and the intensity increase arises from the newly formed amide groups in the maleamic acid units. However, the shape of the 1635 cm^{-1} band is different from that observed in the ATBN spectrum. Its position corresponds to that of hydrogen-bonded amide carbonyls, although the frequency is 7 cm^{-1} lower than that of the same mode in the ATBN spectrum; furthermore, it is very sharp (fwhh = 15 cm^{-1}) and rather symmetrical. These observations, along with the shift of amide band II by 30 cm^{-1}, indicate that the molecular interactions realized by the maleamic acid moieties of AMTBN are different and stronger than those oc-

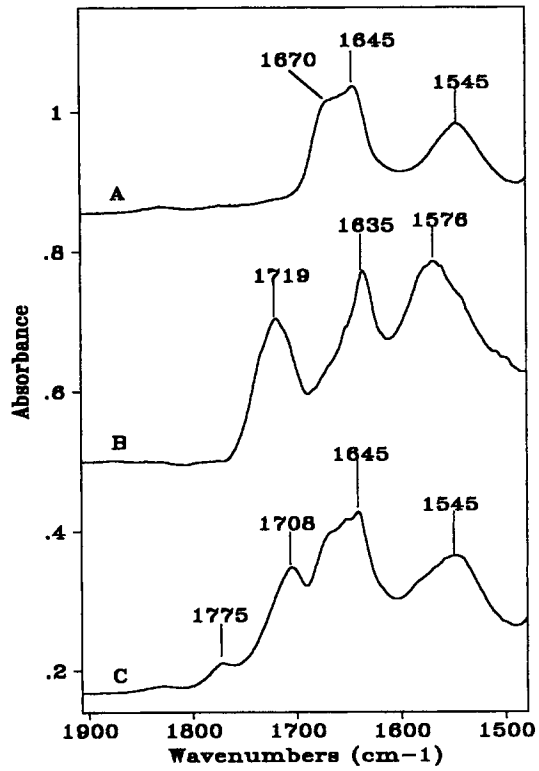

Figure 2 FTIR transmission spectra in the frequency range 1900–1500 cm^{-1} of (A) ATBN, (B) MATBN, and (C) ITBN.

curring among the amide linkages present in the terminal groups of ATBN. The symmetry of the 1719 and the 1635 cm^{-1} peaks also indicate that the vast majority of maleamic acid groups are involved in the same kind of molecular interactions.

Finally, the FTIR spectrum of ITBN [Fig. 1(C)] clearly shows the occurrence of the cyclization process. The ν_{NH} absorption decreases as a consequence of the consumption of the NH groups of the maleimide. The $\nu_{C=O}$ peak centered at 1719 cm^{-1} in the MATBN spectrum is shifted at 1708 cm^{-1} and its intensity is enhanced; a satellite band appears as a shoulder of the main $\nu_{C=O}$ absorption at 1775 cm^{-1}. This doublet is characteristic of imides and is due to the in-phase and out-of-phase stretching vibration of the imide carbonyls, respectively. As expected, both amide bands I and II decrease in intensity down to the values originally found in the ATBN spectrum.

It has been already mentioned that the cyclization reaction also proceeds at temperatures above 100°C. Since the cyclization of the maleamic acid end groups produces well-detectable features in the infrared spectrum, FTIR spectroscopy represents a particularly attractive technique to follow the kinetics of such a process. To this end, a thin film (≈ 5 μm) of MATBN was subjected to thermal cyclization in a temperature chamber directly mounted in the FTIR spectrometer. Infrared spectra were recorded at fixed time intervals for the real-time monitoring of the process during the isothermal experiment; the collected spectral data are reported in Figure 3(A) and (B).

The gradual decrease with time of the absorbencies at 3270, 1632, and 1558 cm^{-1} is evident (depletion of the amide groups). Concurrently, the peak originally centered at 1719 cm^{-1} gradually shifts at 1710 cm^{-1} and increases in intensity, and a satellite band at 1775 cm^{-1} develops (formation of imide rings).

From the above spectral data, it is possible to evaluate the relative conversion of maleamic acid groups as a function of the reaction time using as analytical peak the one centered at 1632 cm^{-1}. The α vs. time curve relative to the process carried out at 125°C is reported in Figure 4; it is observed that, at this temperature, complete cyclization is approached in about 100 min.

The spectrum of the thermally cyclized ITBN is very close to that of the ITBN obtained by the solution reaction. However, while the latter product remains soluble in all the solvents of the rubber, the former is completely insoluble. Evidently, a crosslinking reaction occurs at temperatures of 125°C or above, which is not detected spectroscopically. Such a process is likely to involve the bismaleimide unsaturations which could be thermally activated owing to their very high reactivity.

The bismaleimide double bonds give very weak signals in the IR spectrum and, being present as terminal groups, their concentration is very low. This accounts for the fact that no detectable differences are observed between the spectra of soluble and insoluble products. In this context, a further relevant observation is that, unlike the ATBN copolymer which remains stable, the ITBN prepared by the solution method becomes insoluble when treated at 125°C. This confirms that the crosslinking involves the maleimide groups and suggests that during the thermal ring-closure process cyclization and cross-linking occur simultaneously.

Morphological Analysis of UP-based Blends

Ultrathin sections of UP/ATBN and UP/ITBN blends stained with osmium tetroxide were examined by transmission electron microscopy (TEM) to obtain information on the internal structure of the

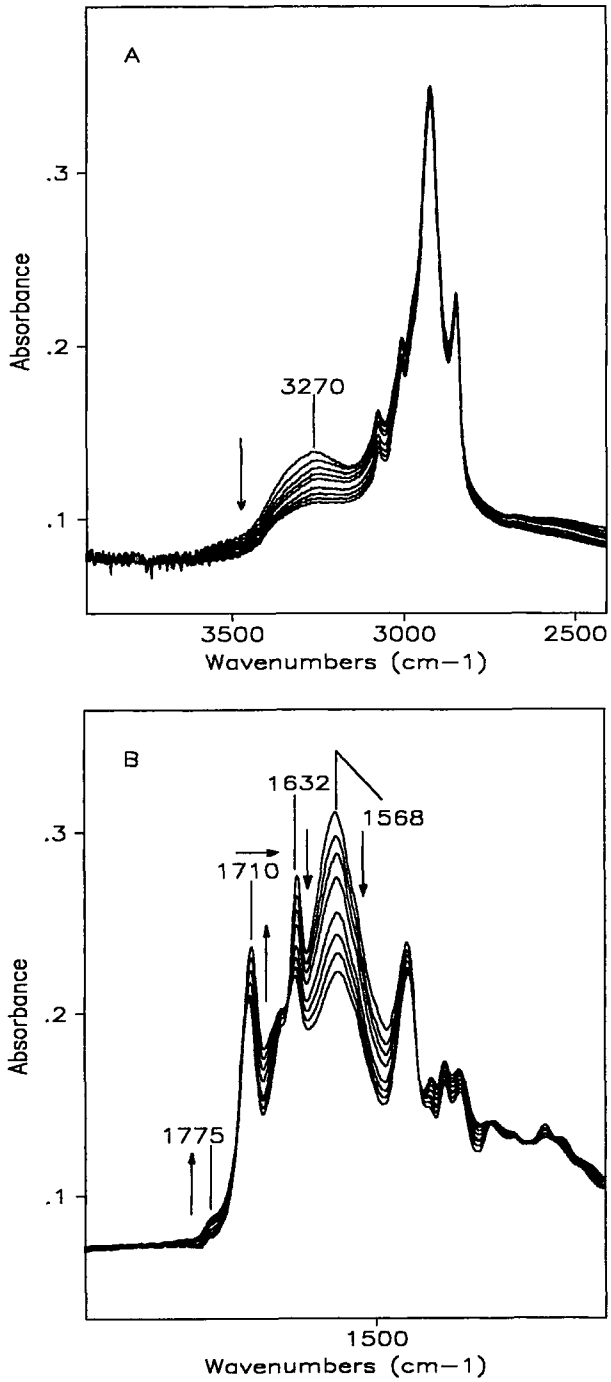

Figure 3 Real-time spectroscopic monitoring of the cyclization reaction of MATBN at 125°C: (A) frequency range 3900–2400 cm^{-1}; (B) frequency range 2000–1100 cm^{-1}. The up and down arrows in the figures indicate, respectively, absorbance increase and decrease with reaction time.

rubber particles. Both ATBN and ITBN contain unsaturated sites along their backbone and are therefore dark-stained in the presence of osmium tetraoxide, giving a good contrast with the saturated UP matrix. This is clearly shown in Figures 5 and 6 where TEM micrographs of UP/ATBN and UP/ITBN blends containing 10% by weight of rubber are reported.

For both types of the modifier, the rubbery phase shows a spherical shape, indicating that no deformation of the rubbery domains during sectioning has occurred. However, most of the ATBN particles appear detached from the UP matrix, while all the ITBN domains remain well bonded to the matrix. This is an indication that better adhesion between the two phases is attained in the UP/ITBN system. The stained ATBN particles (see Fig. 5) show a very coarse internal structure in contrast with the relatively fine and homogeneous texture exhibited by the ITBN particles.

Moreover, both ATBN and ITBN particles do not seem to contain inclusions of UP resin, indicating that the dispersed phase is made solely of the rubber component. The size of the rubber domains is the same for both the blend systems investigated and ranges from 5 to 10 μm. To obtain further details on the nature and distribution of these rubber particles, fracture surfaces obtained by breaking the blend samples in liquid N_2 were examined by scanning electron microscopy (SEM). Prior to the SEM observation, the fracture surfaces were etched with a solvent of the rubber component (CH_2Cl_2).

Figure 7 shows the micrographs of the UP resin modified with 10% of ATBN and ITBN. Comparing the micrographs, it appears that the etching treatment removes completely most of the ATBN particles [see Fig. 7(A)], leaving cavities uniformly dis-

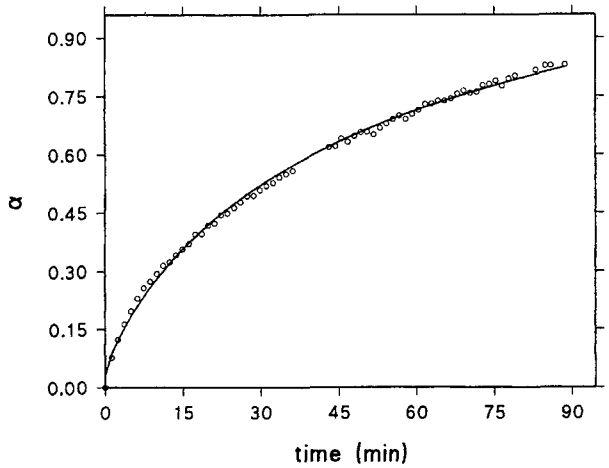

Figure 4 Relative conversion, α, of the maleamic acid end groups of MATBN as a function of the reaction time for the process carried out at 125°C.

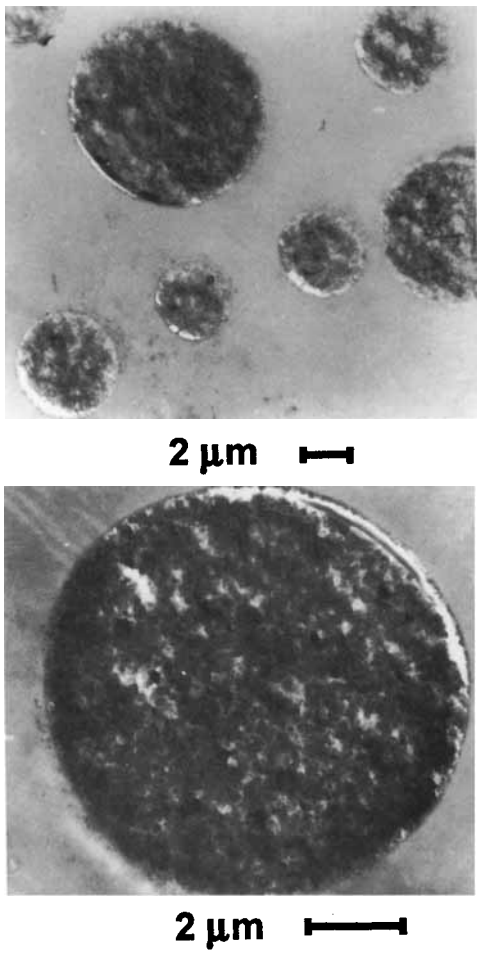

Figure 5 TEM micrographs of a stained ultrathin section of the B10 blend.

tributed within the matrix. In contrast, the fracture surface of the UP/ITBN blend remains almost completely unaffected by the etching treatment [see Fig. 7(B)], thus indicating that the ITBN domains, after the curing process, are no longer soluble in CH_2Cl_2, likely because a crosslinking reaction of the rubber has occurred. The FTIR results discussed in the previous paragraph indicated that the ITBN is readily crosslinked at temperatures above 120°C through a radical process involving the maleimide end groups. The curing process of the blend is carried out at lower temperatures but in the presence of a peroxide catalyst which could also initiate the ITBN crosslinking process. Crosslinked rubbery domains would exhibit a higher stiffness, and this could account for the finer texture observed in the TEM analysis, which is likely due to a more efficient microsectioning of the rubber particles in the UP/ITBN system with respect to the UP/ATBN blend.

Furthermore, once formed, the ITBN macroradicals may also interact at the interface with the UP/styrene system being cured. In such a case, some ITBN molecules would be firmly bonded to the UP/styrene network, thereby improving the interfacial adhesion among the phases. This improvement, in turn, will play an important role in determining the low and the large strain properties of the UP/ITBN blend system. In the next paragraphs, we show evidence indicating the both the ITBN reactions mentioned above do occur simultaneously.

Chemical interactions occurring in the UP/ITBN system during the curing process were further confirmed by selective extraction of the blend components. The blends were first finely ground and then left in CH_2Cl_2 for 48 h; the solvent removes the soluble fraction of the rubber as well as the residual uncrosslinked UP fraction. The quantitative results of such an analysis are reported in Table III. It is noted that in pure UP the amount of unreacted UP molecules is negligible (1.6%).

In the 90/10 UP/ATBN blend, the total soluble fraction amounts to 12.45%. Solution infrared anal-

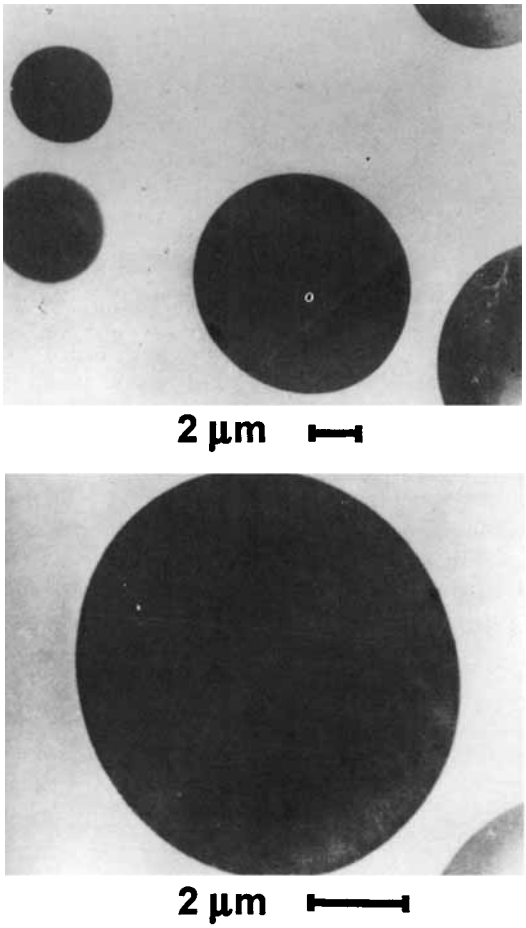

Figure 6 TEM micrographs of a stained ultrathin section of the C10 blend.

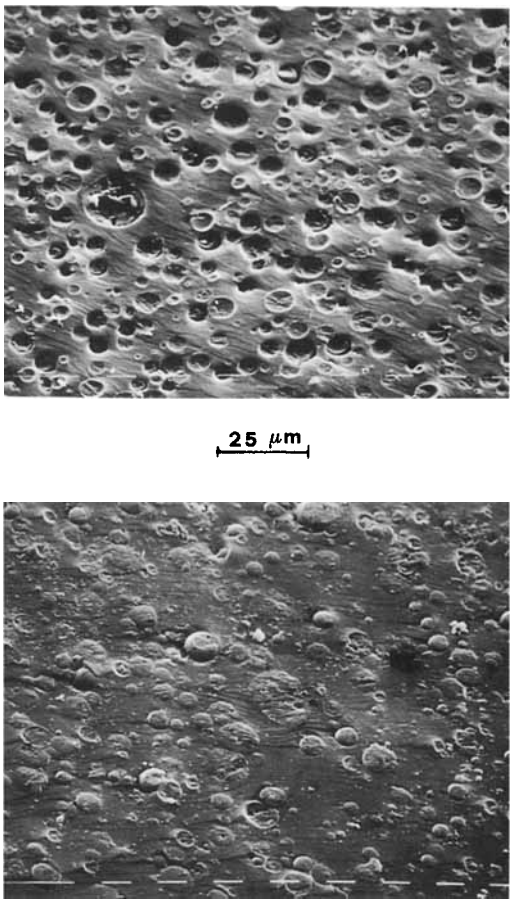

Figure 7 SEM micrographs of the fracture surfaces of samples broken in liquid N_2 and etched in $CHCl_3$: (A) B10 blend; (B) C10 blend.

ysis showed that 9.15% of this fraction is ATBN, while the remaining 3.3% is unreacted UP. Thus, we were able to extract most of the rubber initially present in the blend (91.6%).

On the contrary, in the 90/10 UP/ITBN blend, the total recovered fraction drastically decreases (4.47%) due to the fact that only 15.7% of the initial ITBN content can be extracted. The unreacted UP fraction does not change noticeably (2.9%). Finally, for the 85/15 UP/ITBN blend, we found 9.7% of extractable ITBN and 2.9% of UP.

Modulus and Yield Stress Measurements

The Young's modulus, E, of the various rubber-modified UP resins was determined in three-point bending mode using the equation

$$E = \frac{L^3 P}{4dWB^3} \tag{3}$$

where d is the displacement; P, the load at the displacement d; L, the span; and W and B, the width and the thickness of the specimen, respectively. The E vs. composition curves for both UP/ITBN (curve A) and UP/ATBN (curve B) blends are shown in Figure 8. As expected, for all the materials tested, the modulus decreases gradually with increasing the amount of rubber. In particular, a linear correlation is found between the modulus and composition. It can be noted, however, that the ITBN based blends display higher values of E with respect to the ATBN blends. This apparently surprising result can be explained by assuming that the ITBN rubber undergoes a crosslinking reaction during the curing of the UP matrix. Such a process enhances the ITBN modulus and, therefore, the softening effect of the ITBN rubber is less pronounced than that of the uncrosslinked ATBN rubber.

To predict large-strain properties, the yielding behavior of all the investigated blends was examined under an uniaxial compression mode. Typical stress–strain curves obtained at the same loading rate and temperature as for the Young's modulus are shown in Figures 9 and 10 for UP/ATBN and UP/ITBN blends, respectively. It can be observed that, when loaded in compression, all the samples yield and flow, contrary to what appears in tension,[13] where they exhibit a completely brittle behavior. For convenience, all the stress–strain curves have been re-

Table III Results of the Selective Extraction of the Blend Components

Code	Fraction Extracted (%)	Total Amount of UP Extracted (%)	Total Amount of Rubber Extracted (%)	Amount of Rubber Extracted on the Total Rubber Present in the Blend (%)
B0	1.55	1.55	—	—
B10	12.45	3.30	9.15	91.6
C10	4.47	2.90	1.57	15.7
C15	4.36	2.90	1.45	9.7

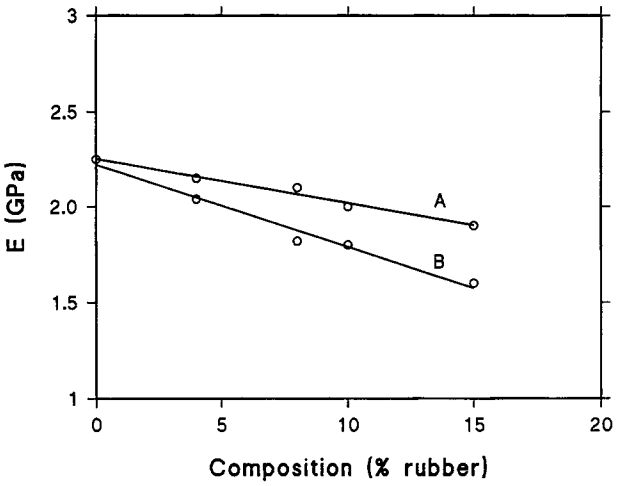

Figure 8 Elastic modulus, E, as a function of blend composition: (A) UP/ITBN system; (B) UP/ATBN system.

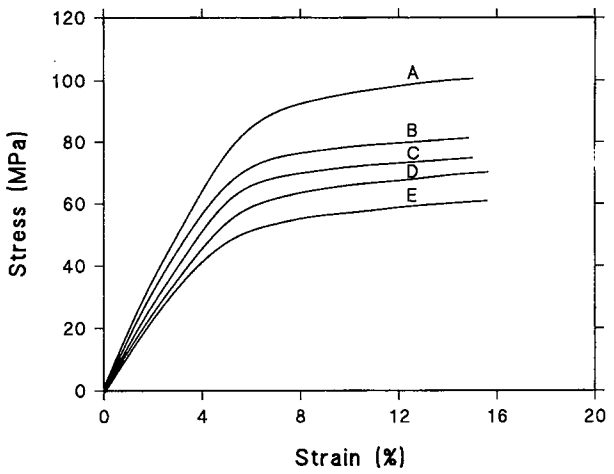

Figure 10 Compressive stress–strain curves at ambient temperature and at a crosshead speed of 1 mm/min for the UP/ITBN system: (A) B0; (B) C4; (C) C8; (D) C10; (E) C15.

ported up to 15% deformation, although some samples were found to deform to strains exceeding 20%.

The compressive yield stress, $\sigma_{c,y}$, evaluated as in Figure 9, is plotted as a function of blend composition in Figure 11. For both UP/ITBN (curve A) and UP/ATBN (curve B), the yield stress decreases with increasing rubber content. This is a direct consequence of the lower shear modulus of the rubbery phase compared to the thermosetting matrix, which prevents the rubber domains to support a significant amount of the applied stress.

From Figure 11 it is also evident that, in the composition range investigated, the UP/ITBN system exhibits higher $\sigma_{c,y}$ values with respect to the UP/ATBN blend. This behavior is generally observed whenever an improved adhesion is realized between the matrix and the dispersed phase. In fact, in such a case, the rubbery domains are able to act as load-bearing components due to the mechanical continuity of the structure. Thus, larger stresses are

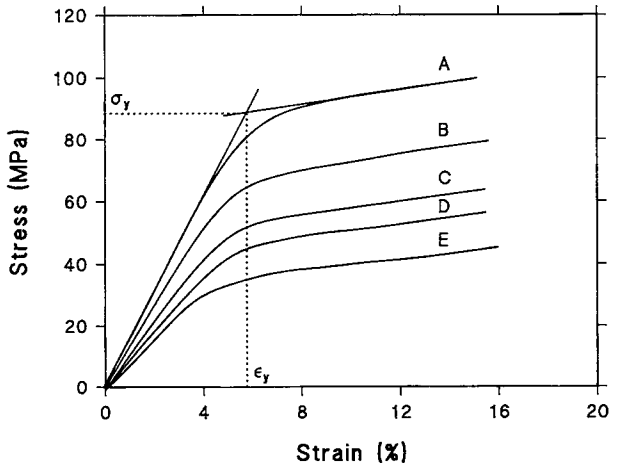

Figure 9 Compressive stress–strain curves at ambient temperature and at a crosshead speed of 1 mm/min for the UP/ATBN system: (A) B0; (B) B4; (C) B8; (D) B10; (E) B15.

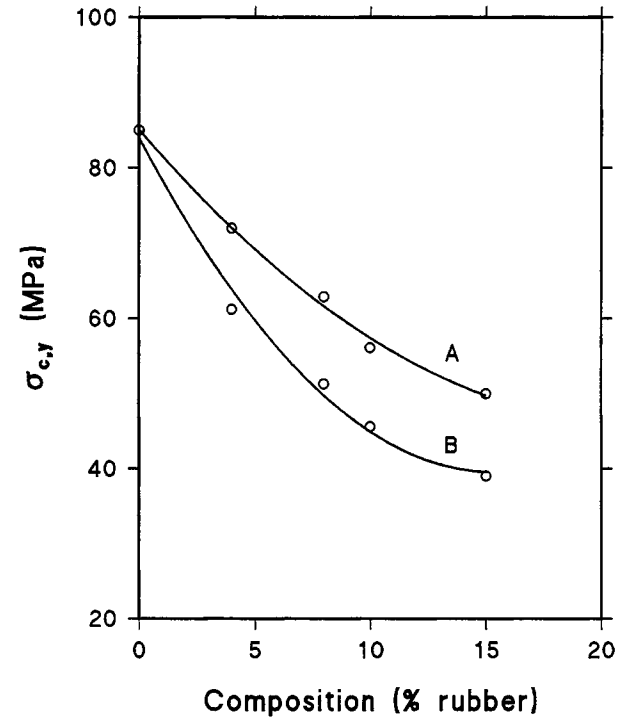

Figure 11 Compressive yield stress, $\sigma_{c,y}$, as a function of blend composition: (A) UP/ITBN system; (B) UP/ATBN system.

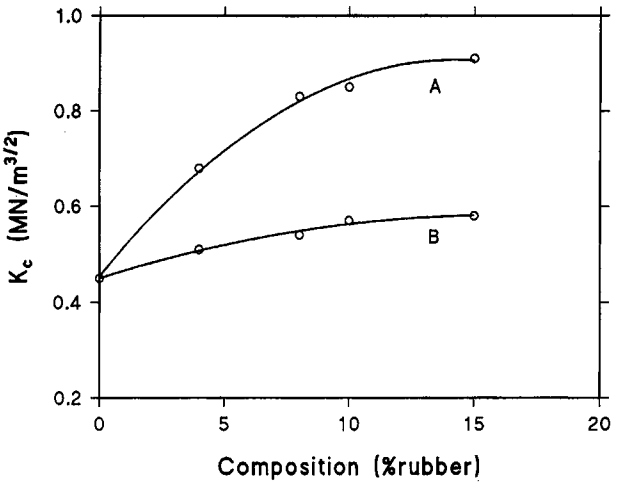

Figure 12 Critical stress intensity factor, K_c, at low strain rate (1 mm/min), as a function of blend composition: (A) UP/ITBN system; (B) UP/ATBN system.

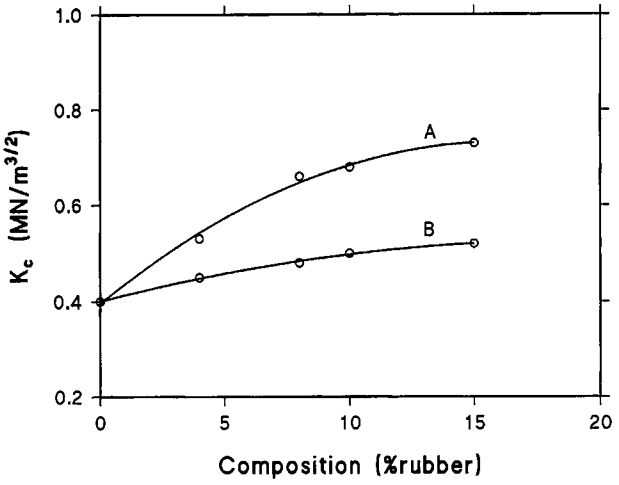

Figure 14 Critical stress intensity factor, K_c, under impact conditions (1 m/s) as a function of blend composition: (A) UP/ITBN system; (B) UP/ATBN system.

needed to yield the material. The better adhesion realized in the UP/ITBN system may arise from the chemical interaction between the maleimide functionalities of ITBN and the unsaturations of the UP/styrene system during the curing process.

Fracture Behavior

On samples cured at 70°C and postcured at 100°C, fracture mechanics tests at low and high deformation rates were performed to evaluate the intrinsic toughness. For both plain and rubber-modified resins tested at a low deformation rate (1 mm/min), the critical stress intensity factor, K_c, determined from the load-displacement curves using eq. (1) is reported in Figure 12 as a function of the rubber content in the blend. It can be seen that, while in the case of the UP/ATBN system (curve B) the K_c increase is relatively modest, for the UP/ITBN system (curve A), a substantial enhancement of toughness is found. In particular, K_c increases sharply by addition of small amounts of ITBN rubber and than levels off at a rubber content of 10–15%. The enhanced toughness showed by this blend system is further evidenced in Figure 13, where the fracture data are expressed by the parameter G_c (critical strain energy release rate). The values of G_c were calculated from the values of K_c and of the elastic modulus E, according to the equation

$$G_c = \frac{K_c^2}{E}(1 - \nu^2) \tag{4}$$

where ν is the Poisson's ratio, taken as 0.35. In terms of G_c, the addition of 10–15% of the modifier increases the toughness of the UP matrix by a factor of about 5 when the rubber is ITBN and of about 2 in the case of ATBN.

Fracture measurements were also carried out under impact conditions (1 m/s) in order to evaluate the toughness of these materials under rapid loading. The corresponding K_c and G_c values are reported in Figures 14 and 15, respectively. Here, the K_c values were obtained as previously using eq. (1), while the G_c values were estimated either by energy measurements according to eq. (2) or from the corresponding K_c and E values according to the eq. (4).

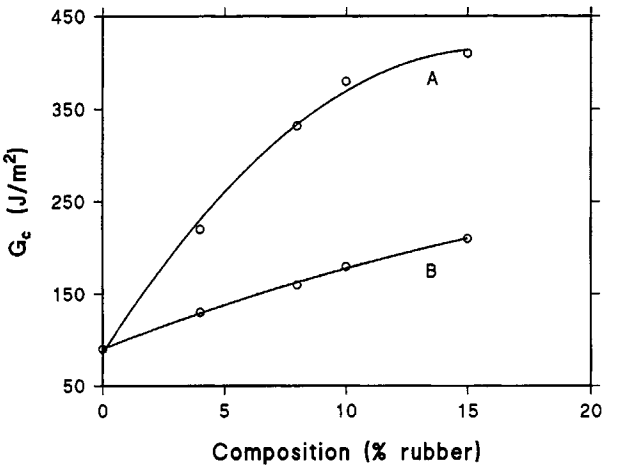

Figure 13 Critical strain energy release rate, G_c, at low strain rate (1 mm/min) as a function of blend composition: (A) UP/ITBN system; (B) UP/ATBN system.

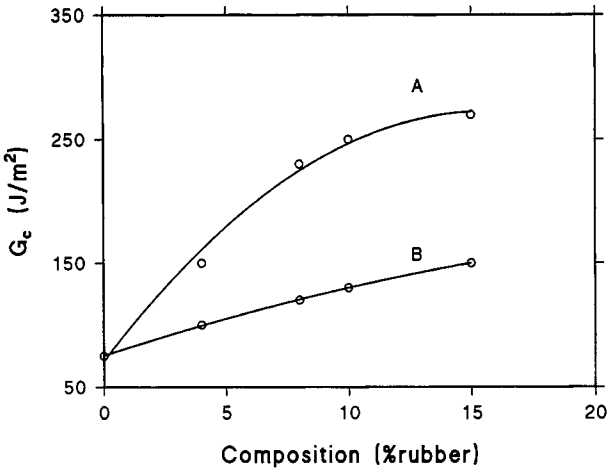

Figure 15 Critical strain energy release rate, G_c, under impact conditions (1 m/s) as a function of blend composition: (A) UP/ITBN system; (B) UP/ATBN system.

The elastic modulus E used in eq. (4) was determined at an impact speed comparable to that used in the fracture measurements by means of rebound tests.[14,15] The G_c values determined by the above methods were practically coincident.

The behavior of the impact toughness parameters is analogous to that observed in the low-speed tests, apart from a decrease in the absolute values of K_c and G_c. A reduction of toughness on increasing the loading rate is a general phenomenon related to the reduced capacity of viscoelastic and plastic deformation which polymeric materials exhibit when the strain rate is enhanced.

The whole of the fracture data clearly evidence the higher toughening efficiency of the ITBN rubber with respect to ATBN. According to the currently accepted toughening theories on multicomponent thermosetting systems,[16–18] during loading, in both the ATBN- and ITBN-modified resins, the rubber particles produce stress concentration at their equators and these act as sites for the initiation and growth of localized shear deformation in the matrix. This mechanism is believed to be the main source of energy dissipation and occurs to a greater extent in the UP/ITBN blend mainly because of the stronger adhesion across the particle–matrix interface, which prevents premature particle debonding. In fact, when a good adhesion is realized, the rubbery domains are able to act as load-bearing components due to the continuity of the structure. Thus, extensive shear yielding can be formed in front of the crack tip which can absorb a large amount of energy before the final fracture occurs. This process is strongly reduced when there is poor or no adhesion at the particle/matrix interface.

Further details on the deformation mechanism occurring in these blend systems were obtained by a fractografic analysis of the surfaces of samples fractures at a low deformation rate. In Figure 16 are shown the SEM micrographs of an UP/ATBN and an UP/ITBN containing 10% by weight of the modifier. The micrographs were taken near the notch tip, in the region of crack growth. The micrograph of the UP/ATBN blend [Fig. 16(A)] reveals that the majority of the rubber particles have been fractured approximately along their equatorial plane. The average diameter of these particles appears to be unchanged, within experimental uncertainty, compared to the diameter of the undeformed particles as determined by TEM. This seems to indicate that the fracture of the rubber domains occurs without particle cavitation. However, some unbroken particles clearly debonded from the matrix are also observed. The above findings, together with the relative smoothness of the fracture surface around the rubber particles, indicate that no significant plastic deformation has occurred ahead the crack tip. The other UP/ATBN blend compositions investigated (mi-

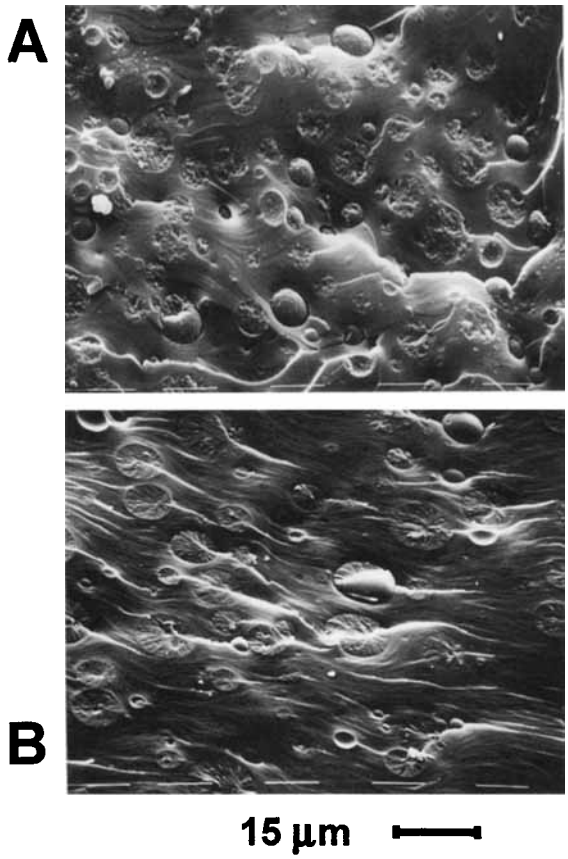

Figure 16 SEM micrographs of fracture surfaces obtained at low strain rate: (A) B10 blend; (B) C10 blend.

crographs not reported) display analogous fractografic features.

When ATBN is replaced by ITBN [Fig. 16(B)], we again observe equatorial rupture of the rubber particles, but there is no evidence for particle debonding. Moreover, the fracture surface displays clear evidence of extensive plasticity of the UP matrix.

The fractografic analysis is in agreement with the toughness results and gives conclusive evidence that the primary source of energy dissipation is the formation of a plastic zone ahead the crack tip. In fact, the stress field associated with the rubber particles promote the formation of multiple but localized shear deformation bands in the matrix. Although the two types of rubber investigated display similar particle-size distribution, this mechanism is far more effective in the ITBN-modified resin. This may be related, as already pointed out, to a better adhesion at the particle/matrix interface which is realized in this system through a chemical interaction between the rubber and the UP resin. It is to be noted, however, that a further contribution to energy absorption in the UP/ITBN system arise from the crosslinked structure of the rubber domains which require a higher energy to be broken.

Plastic Zone at the Crack Tip

We have already stressed that localized yielding in the vicinity of the crack-tip is the main mechanism controlling the degree of plastic deformation and the increased toughness of the investigated rubber-modified UP resins. In the light of this observation, it is of interest to examine models which combine yield and fracture data in order to obtain a quantitative estimation of the deformation process occurring at the crack tip. It has been shown[14,19] that, for relatively brittle polymers, the extent and shape of the localized plastic deformation ahead of a crack tip can be successfully described using the models developed by Dugdale[19] and Irwin.[20] The Dugdale model assumes that the yielding of the material at the crack tip renders the crack longer by an amount equal to the length of the plastic zone R. The value of R is related to K_c and to the tensile yield stress σ_y by

$$R = \frac{\pi}{8}\left(\frac{K_c}{\sigma_y}\right)^2 \tag{5}$$

Similarly, Irwin advanced the hypothesis that the shape of the plastic zone ahead the crack tip can be considered approximately circular. From geometrical considerations, he concluded that the radius, r_p, of this zone, can be estimated, for the plain strain case, by

$$r_p = \frac{1}{6\pi}\left(\frac{K_c}{\sigma_y}\right)^2 \tag{6}$$

Comparison of eqs. (5) and (6) reveals that the Dugdale model predicts a larger extent of plasticity than does the Irwin circular model. However, both equations predict that the size of the plastic zone is proportional to $(K_c/\sigma_y)^2$.

The R and r_p values calculated according to eqs. (5) and (6), respectively, are reported as a function of blend composition in Figures 17 and 18, respectively. The tensile yield stress values were obtained from the uniaxial compression tests, assuming the ratio $\sigma_{t,y}/\sigma_{c,y}$ to be equal to 0.75.[21,22] Both the r_p and R parameters increase linearly with increasing the rubber content in the blend, but the values relative to the UP/ITBN blend are higher than those of the UP/ATBN blend. These results further confirm the higher efficiency of the ITBN rubber in toughening the UP resin.

CONCLUSIONS

The NH_2 end groups of a butadiene–acrylonitrile copolymer were transformed into maleimide groups to enhance the reactivity of the copolymer toward an unsaturated polyester matrix. The characterization of the ITBN copolymer was carried out by FTIR

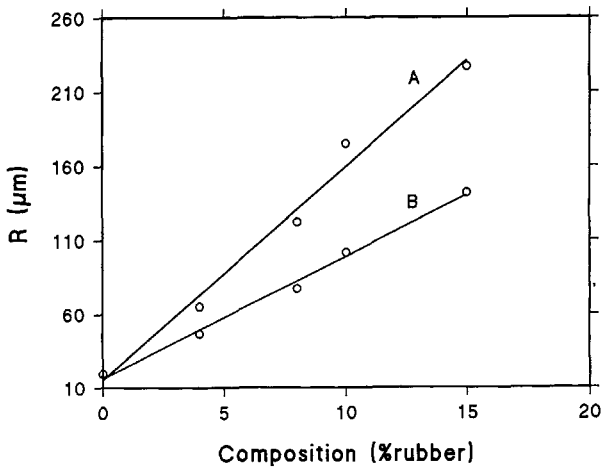

Figure 17 The length of the plastic zone, R, as a function of blend composition: (A) UP/ITBN system; (B) UP/ATBN system.

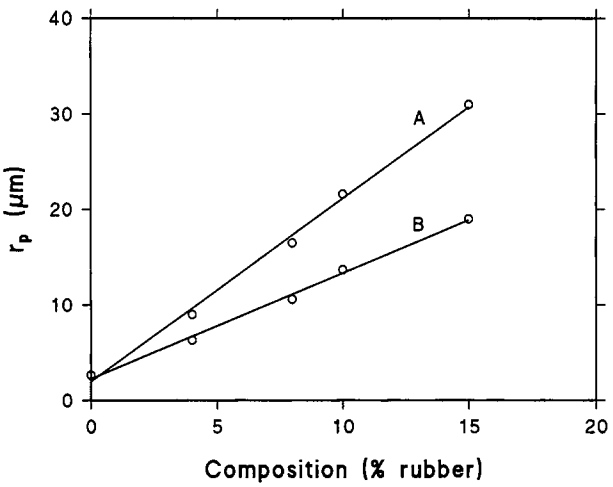

Figure 18 The radius of the plastic zone, r_p, as a function of blend composition: (A) UP/ITBN system; (B) UP/ATBN system.

spectroscopy. The solution reaction between ATBN and maleic anhydride proceeds in two steps: the formation of a maleamic acid intermediate and its cyclyzation via dehydrating agents. The cyclization process was also carried out by a thermal treatment above 120°C and followed by FTIR spectroscopy. It was found that in these conditions ITBN undergoes a crosslinking process initiated by its maleimide end groups.

The mechanical and the fracture properties of a series of blends containing the modified (ITBN) and the unmodified (ATBN) rubber were investigated. Both the modulus and the yield stress decreased upon addition of the rubber component, but this effect was less pronounced for the UP/ITBN blends. Fracture measurements at low and high rates of deformation demonstrated a substantial increase of toughness when ITBN was used as a modifier. These results were ascribed to an improved adhesion among the phases which is realized in the UP/ITBN system because of the occurrence of chemical interactions among the components during the curing process.

The higher efficiency of ITBN as a toughener compared to ATBN was further confirmed by a morphological analysis performed by scanning and transmission electron microscopy. Such an analysis demonstrated that the primary source of energy dissipation in these blend systems is localized shear yielding of the matrix which occurred to a greater extent when ATBN was replaced by ITBN.

Thanks are due to Mr. V. Di Liello for technical assistance in performing the mechanical and fracture measurements and to Mr. G. Orsello for his help in carrying out the morphological analysis. This work was partially supported by C.N.R. "Progetto Finalizzato Chimica Fine II."

REFERENCES

1. J. M. Margolis, Ed., *Advanced Thermoset Composites. Industrial and Commercial Applications,* Van Nostrand Reinhold, New York, 1986.
2. L. Suspene, D. Fourquier, and Y. S. Yang, *Polymer,* **32,** 1593 (1991).
3. K. E. Atkins, in *Polymer Blends,* D. R. Paul and S. Newman, Eds., Academic Press, New York, 1978, Chap. 2, p. 39.
4. C. K. Riew and J. K. Gilham, Eds., *Rubber Modified Thermoset Resins,* Advances in Chemistry and Sciences Series 208, American Chemical Society, Washington, DC, 1984.
5. J. A. Crosbie and M. G. Phillips, *J. Mater. Sci.,* **20,** 563 (1985).
6. A. J. Kinlock, S. J. Shaw, and D. L. Hunston, *Polymer,* **24,** 1355 (1983).
7. E. Martuscelli, P. Musto, G. Ragosta, G. Scarinzi, and E. Bertotti, *J. Polym. Sci.,* **31,** 619 (1993).
8. J. C. Williams, *Fracture Mechanics of Polymers,* Wiley, New York, 1984.
9. W. F. Brown and J. Srawley, ASTM STP4, American Society for Testing and Materials, Philadelphia, 1966, p. 13.
10. E. Plati and J. G. Williams, *Polym. Eng. Sci.,* **15,** 470 (1975).
11. D. J. Skrovanek, S. E. Howe, P. C. Painter, and M. M. Coleman, *Macromolecules,* **18,** 1676 (1985).
12. S. Krimm, *Biopolymers,* **22,** 217 (1983).
13. A. J. Kinloch and R. J. Young, *Fracture Behavior of Polymers,* Applied Science, London, 1983.
14. T. Casiraghi, *Polym. Eng. Sci.,* **23,** 899 (1982).
15. R. Greco and G. Ragosta, *Plast. Rubb. Proc. Appl.,* **7,** 163 (1987).
16. C. B. Bucknall, *Toughened Plastics,* Applied Science, London, 1977.
17. A. F. Yee and R. A. Pearson, *J. Mater. Sci.,* **21,** 2462 (1986).
18. A. J. Kinloch, S. J. Shaw, D. A. Tod, and D. L. Hunston, *Polymer,* **24,** 1341 (1983).
19. D. S. Dugdale, *J. Mech. Phys. Solids,* **8,** 100 (1960).
20. G. R. Irwin, *Appl. Mater. Res.,* **3,** 65 (1964).
21. A. J. Kinloch, S. J. Shaw, and D. L. Hunston, *Polymer,* **24,** 1355 (1983).
22. J. N. Sultan and M. MacGany, *J. Polym. Eng. Sci.,* **13,** 29 (1973).

Received January 5, 1996
Accepted June 10, 1996